Sensor signal processing

Automated Detection of Pulmonary Diseases From Lung Sound Signals Using Fixed-Boundary-Based Empirical Wavelet Transform

Rajesh Kumar Tripathy[1], Shaswati Dash[1], Adyasha Rath[2], Ganapati Panda[3], and Ram Bilas Pachori[4]

[1]*Department of Electrical and Electronics Engineering, Birla Institute of Technology and Science Pilani, Hyderabad Campus, Hyderabad 500078, India*
[2]*Department of Computer Science and Engineering, Siksha O Anusandhan University, Bhubaneswar 751030, India*
[3]*Department of Electronics and Tele-Communication, C. V. Raman Global University, Bhubaneswar 752054, India*
[4]*Department of Electrical Engineering, Indian Institute of Technology Indore, Indore 453552, India*

Manuscript received March 22, 2022; revised April 2, 2022; accepted April 11, 2022. Date of publication April 13, 2022; date of current version April 25, 2022.

Abstract—In this letter, a promising method is proposed to automatically detect pulmonary diseases (PDs) from lung sound (LS) signals. The modes of the LS signal are evaluated using empirical wavelet transform with fixed boundary points. The time-domain (Shannon entropy) and frequency-domain (peak amplitude and peak frequency) features have been extracted from each mode. The classifiers, such as support vector machine, random forest, extreme gradient boosting, and light gradient boosting machine (LGBM), have been chosen to detect PDs using the features of LS signals automatically. The performance of the proposed method has been evaluated using LS signals obtained from a publicly available database. The detection accuracy values, such as 80.35, 83.27, 99.34, and 77.13%, have been obtained using the LGBM classifier with fivefold cross validation for normal versus asthma, normal versus pneumonia, normal versus chronic obstructive pulmonary disease (COPD), and normal versus pneumonia versus asthma versus COPD classification schemes. For the normal versus pneumonia versus asthma classification scheme, the proposed method has achieved an accuracy value of 84.76%, which is higher than that of the existing approaches using LS signals.

Index Terms—Sensor signal processing, accuracy, classifiers, empirical wavelet transform (EWT), lung sound (LS), pulmonary diseases (PDs).

I. INTRODUCTION

The stethoscope is used as an essential diagnostic instrument for diagnosing heart valve diseases and pulmonary diseases (PDs) in clinical studies [1]. The invention of the digital stethoscope enables the continuous recording of lung sound (LS) data from the subjects for the automated detection of various PDs [2]. The diseases, such as chronic obstructive pulmonary disease (COPD), asthma, pneumonia, bronchitis, and pulmonary fibrosis, are diagnosed using LS signals [3]. The presence of abnormal sounds, such as wheezes, crackles, and rhonchi, is the symptom of the diagnosis of various PDs [4]. The automated analysis of LS signals is, thus, vital for accurately detecting PDs [2]. The automated systems evaluate features from the LS signals and use these features as input to different machine learning algorithms to detect PDs. Developing new approaches for the automated detection of PDs from LS data is an exciting research topic in healthcare engineering.

Over the last decade, various artificial-intelligence-based algorithms have been used to classify normal and abnormal LS signals [5]. The short-time Fourier transform (STFT) [6], wavelet-based [6], and Mel-frequency cepstral coefficient (MFCC) features [7] combined with different classifiers have been used to classify normal and abnormal LS signals. Similarly, the STFT-based time–frequency images of LS signals and the convolutional support vector machine (SVM) have also been used to detect normal and abnormal LS classes [8]. The convolutional neural network (CNN) has been used for the automated classification of normal and abnormal LS signals [9]. Recently, Shi *et al.* [10] have proposed the visual-geometry-group-network-based transfer learning and the bidirectional gated recurrence unit model for the automated detection of pneumonia and asthma using the time–frequency domain images of LS signals. It is observed from the reported literature that the MFCC, STFT, and wavelet-based methods have demonstrated less classification performance for the automated detection of PDs using LS signals. In addition, the existing methods have not considered the hidden information from the different frequency components of the LS signals to detect PDs. Moreover, the deep learning methods used in [8] and [10] have achieved less classification accuracy to detect abnormal LS components. Thus, there is an opportunity to develop improved methods to detect PDs using LS signals.

The empirical wavelet transform (EWT) with fixed boundary points (FBPs) has been introduced in [11] to decompose the electrocardiogram signal into components or modes. This method uses FBPs instead of the local maxima- or minima-based boundary point detection in the Fourier spectrum of the signal to design the empirical wavelet filter bank [12]. The EWT with FBPs has not been applied to analyze normal and pathological LS signals. Similarly, the gradient boosting machine (GBM)-based machine learning models have rarely been used for different biomedical applications [13], [14]. Particularly, these models have not been explored to detect PDs using the features of LS signals. The novelty of the proposed work is to determine the time- and frequency-domain features from the multiscale analysis of LS signals and employ GBM models to achieve the detection of PDs.

II. DETAILS OF THE LS DATABASE

In this letter, a public database [15] is chosen to evaluate the efficacy of the proposed method for the detection of PDs using LS signals. The

Corresponding author: Rajesh Kumar Tripathy (e-mail: rajeshiitg13@gmail.com).
Associate Editor: S. Kia.
Digital Object Identifier 10.1109/LSENS.2022.3167121

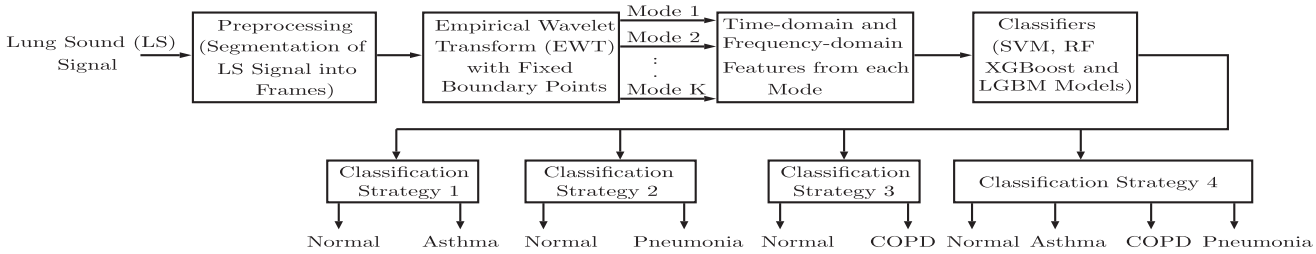

Fig. 1. Block diagram of the proposed approach for the detection of PDs using LS signals.

database consists of 336 LS signals from 112 subjects (35 normal and 77 abnormal) with the age ranging from 50.5 ± 19.40. The sampling frequency of each LS signal is taken as 4 kHz. The abnormal LS signals have been recorded from subjects with asthma, pneumonia, COPD, heart failure, lung fibrosis, and pleural effusion pathologies. The current investigation has employed 96, 27, 15, and 105 LS recordings for asthma, COPDs, pneumonia, and normal classes, respectively, to assess the potentiality of the proposed method.

III. PROPOSED METHOD

The block diagram of the proposed automated PD detection scheme is shown in Fig. 1. The preprocessing step includes the segmentation of each LS signal into frames. The segmentation of the LS signal into frames is performed using a nonoverlapping window. In this study, we have considered different window lengths, such as 4 and 5 s, for the segmentation of LS signals. The optimal window length is chosen based on the final detection performance of the proposed method. The numbers of 5-s duration frames evaluated for normal, asthma, COPD, and pneumonia classes are given as 503, 444, 129, and 105, respectively.

A. EWT With FBPs

The EWT with FBPs is chosen to evaluate modes from the LS signal. In the dyadic wavelet transform (DWT), the spectrum of the analyzed signal is segregated into dyadic grids or subbands based on the number of decomposition levels [12]. However, in the EWT, the filter bank is designed based on the segmentation of the Fourier spectrum of the signal [12]. Then, the designed filter bank is used to compute the components or modes. In this study, the FBPs are used to segment the Fourier spectrum of the LS signal to design a filter bank. The frequency points selected on the spectrum of the LS signal are given as $f_1{:}20{:}f_L$, where $f_1 = 20$ and $f_L = 1000$ are the first and last frequency points, respectively. The factor 20 is denoted as the incremental factor. The frequency points $f_1{:}20{:}f_L$ divide the spectrum of LS signals into 51 contiguous segments, and each segment has a bandwidth of 20 Hz. For the first segment (frequency range as [0, 20 Hz]), the filter frequency response is obtained using the empirical scaling function, but for subsequent segments, these are obtained using the empirical wavelet function [11]. The modes are computed based on the multiplication of the Fourier spectrum of the LS signal with the impulse responses of the filter bank followed by the inverse DFT [12]. The LS signals for normal and pneumonia classes are shown in Fig. 2(a) and (f), respectively. Similarly, the first four modes of LS signals computed using the EWT with FBPs for normal and pneumonia classes are depicted in Fig. 2(b)–(e) and (g)–(j), respectively. It is observed that there are differences in the signal characteristics for normal and pneumonia classes. Significant differences are also noticed in the characteristics of each mode for normal and pathological (pneumonia)

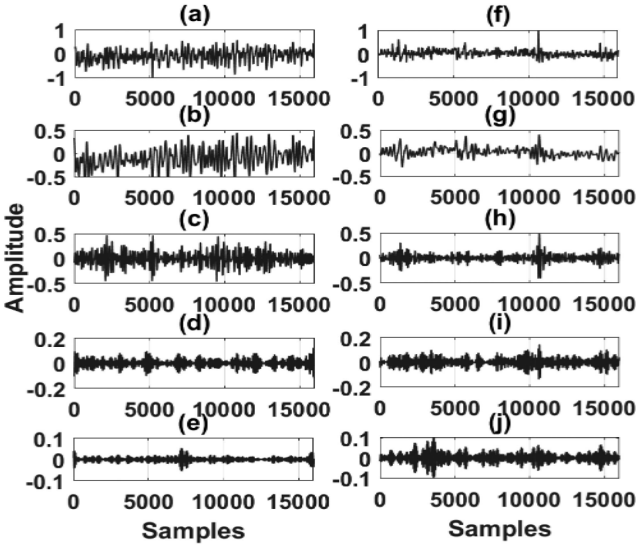

Fig. 2. (a) LS signal for the normal class. (b)–(e) First four modes of the LS signal evaluated using the EWT with FBPs for the normal class. (f) LS signal for the pneumonia class. (g)–(j) First four modes of the LS signal evaluated using the EWT with FBPs for the pneumonia class.

classes. Therefore, the features from the modes of LS signals can be employed for the automated detection of PDs.

B. Extraction of Features and Classification of PDs

In this letter, time- and frequency-domain features have been evaluated from each mode of the LS signal. In the time domain, Shannon entropy from each mode of the LS signal is computed using the histogram of each mode with a bin size of 20. Similarly, for each mode of the LS signal, the spectral peak amplitude and the peak frequency are determined. For each LS frame, 51 modes are obtained. Similarly, three features (one time domain and two frequency domains) are also evaluated. Thus, a 153-D feature vector (FV) is extracted from each LS signal frame. In the same way, the 153-D FV is evaluated for all the LS signal frames at normal, COPD, asthma, and pneumonia classes. The k-nearest neighbor (KNN), multilayer perceptron (MLP), random forest (RF), SVM, extreme gradient boosting (XGBoost), and light gradient boosting machine (LGBM) classifiers [13], [14], [16] are used to detect PDs using 153-D FVs of all the LS signals. The binary classification schemes, such as normal versus asthma, normal versus COPD, and normal versus pneumonia, are considered. Similarly, the four-class classification tasks carried out are normal, pneumonia, asthma, and COPD. The performance of each four classifiers is evaluated using holdout validation (75% instances as training and 25% instances as testing) and fivefold cross-validation (CV) methods [2].

TABLE 1. Performance of Different Classifiers Evaluated Using All the Features of LS Signals With Holdout Validation and Fivefold CV

Classification Scheme	Classifiers	Train/Test Selection	Accuracy	Sensitivity	Specificity	Kappa
Normal versus Asthma	KNN	Hold-out	54.94 ± 2.42	81.56 ± 3.54	34.29 ± 6.11	0.05 ± 0.06
		5-fold	48.14 ± 3.45	80.11 ± 4.70	37.37 ± 5.53	−0.01 ± 0.05
	MLP	Hold-out	51.78 ± 6.27	61.06 ± 45.63	45.56 ± 47.91	0.04 ± 0.04
		5-fold	48.14 ± 3.45	33.60 ± 47.02	64.71 ± 48.32	−0.01 ± 0.05
	SVM	Hold-out	61.61 ± 1.97	69.39 ± 4.47	53.19 ± 6.95	0.22 ± 0.04
		5-fold	64.19 ± 4.23	67.96 ± 6.02	59.89 ± 4.57	0.27 ± 0.08
	RF	Hold-out	73.36 ± 2.31	82.73 ± 2.74	63.26 ± 3.37	0.46 ± 0.04
		5-fold	77.08 ± 2.99	87.68 ± 3.16	65.08 ± 4.42	0.53 ± 0.06
	XGBoost	Hold-out	72.42 ± 1.68	77.01 ± 4.38	67.67 ± 4.95	0.44 ± 0.03
		5-fold	73.39 ± 3.21	77.73 ± 3.63	68.47 ± 4.34	0.46 ± 0.06
	LGBM	Hold-out	77.99 ± 1.63	82.76 ± 4.42	72.99 ± 3.47	0.55 ± 0.03
		5-fold	80.35 ± 3.78	84.88 ± 4.21	75.23 ± 3.49	0.60 ± 0.07
Normal versus COPD	KNN	Hold-out	61.21 ± 11.66	89.80 ± 5.23	34.23 ± 10.13	0.07 ± 0.09
		5-fold	67.78 ± 4.88	90.50 ± 3.70	31.01 ± 9.03	0.24 ± 0.15
	MLP	Hold-out	59.09 ± 7.42	66.67 ± 37.26	55.17 ± 38.80	0.14 ± 0.11
		5-fold	67.78 ± 4.88	90.00 ± 16.95	33.32 ± 30.46	0.24 ± 0.15
	SVM	Hold-out	75.95 ± 4.30	89.08 ± 4.78	56.16 ± 7.09	0.47 ± 0.09
		5-fold	79.33 ± 2.22	86.50 ± 2.85	68.24 ± 8.64	0.55 ± 0.05
	RF	Hold-out	75.54 ± 4.20	89.23 ± 3.77	56.49 ± 8.57	0.46 ± 0.09
		5-fold	77.50 ± 4.11	88.50 ± 3.35	60.39 ± 7.37	0.50 ± 0.09
	XGBoost	Hold-out	78.48 ± 2.91	86.38 ± 4.99	68.88 ± 7.07	0.55 ± 0.05
		5-fold	81.16 ± 7.28	87.00 ± 5..96	72.15 ± 10.87	0.59 ± 0.15
	LGBM	Hold-out	81.81 ± 4.79	89.49 ± 6.51	72.24 ± 8.33	0.62 ± 0.09
		5-fold	83.27 ± 2.44	89.50 ± 4.10	73.66 ± 7.31	0.64 ± 0.05
Normal versus Pneumonia	KNN	Hold-out	73.76 ± 18.36	93.91 ± 2.81	100.00 ± 0.00	0.44 ± 0.28
		5-fold	74.42 ± 11.45	92.50 ± 3.53	100.00 ± 0.00	0.37 ± 0.37
	MLP	Hold-out	73.44 ± 9.08	99.31 ± 1.54	31.36 ± 27.57	0.33 ± 0.28
		5-fold	74.42 ± 11.45	82.00 ± 20.570	60.00 ± 54.77	0.37 ± 0.37
	SVM	Hold-out	100.00 ± 0.00	100.00 ± 0.00	100.00 ± 0.00	1.00 ± 0.00
		5-fold	100.00 ± 0.00	100.00 ± 0.00	100.00 ± 0.00	1.00 ± 0.00
	RF	Hold-out	100.00 ± 0.00	100.00 ± 0.00	100.00 ± 0.00	1.00 ± 0.00
		5-fold	100.00 ± 0.00	100.00 ± 0.00	100.00 ± 0.00	1.00 ± 0.00
	XGBoost	Hold-out	99.01 ± 0.89	98.26 ± 1.61	100.00 ± 0.00	0.97 ± 0.01
		5-fold	97.70 ± 1.86	96.50 ± 2.85	100.00 ± 0.00	0.95 ± 0.04
	LGBM	Hold-out	99.67 ± 0.73	99.31 ± 1.54	100.00 ± 0.00	0.99 ± 0.01
		5-fold	99.34 ± 0.89	99.00 ± 1.36	100.00 ± 0.00	0.98 ± 0.01

The optimal parameters of each classifier are selected using the grid search method [16]. The performance measures, such as sensitivity, specificity, accuracy, and Kappa score, are evaluated for each classifier to detect PDs [16].

IV. RESULTS AND DISCUSSION

The classification results of KNN, MLP, SVM, RF, XGBoost, and LGBM models evaluated using the features of LS signals for holdout validation and fivefold CV are listed in Table 1. It is observed that for normal versus asthma and normal versus COPD classification strategies, the LGBM classifier yields higher accuracy, sensitivity, specificity, and Kappa values compared with XGBoost, RF, SVM, MLP, and KNN classifiers. However, the SVM and RF classifiers have achieved 100% accuracy for the normal versus pneumonia classification case. Similarly, in the case of fivefold CV, similar results have been obtained using SVM, RF, XGBoost, and LGBM classifiers using the features of LS signals for the detection of PDs. It is found that for the normal versus asthma case, the LGBM has demonstrated superior classification performance compared to the other classification models. Similarly, for the normal versus COPD cases, both the XGBoost and LGBM classifiers have achieved more than 80% classification accuracy using the features of LS signals. Moreover, for the fivefold CV of the four-class classification scheme, the accuracy values achieved by SVM, RF, XGBoost, and LGBM models evaluated using the features of LS signals are shown in Fig. 3. It is observed that for fold 1 and fold 2, the accuracy values are higher for the XGBoost model than those of other classification models. Similarly, for fold 3, fold

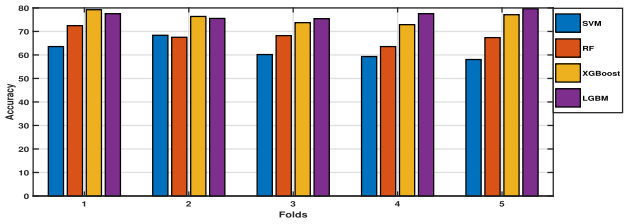

Fig. 3. Comparison of the accuracy values of SVM, RF, XGBoost, and LGBM models for four-class output using fivefold CV.

4, and fold 5, the LGBM has achieved higher accuracy values for the automated detection of PDs using features from LS signals. The optimal parameters of the SVM classifier are obtained as $C = 0.01$, and one value is the radial basis function kernel. The number of nearest neighbors and the number of hidden neurons for KNN and MLP classifiers are considered as 10 and 120, respectively. For the RF classifier, the number of trees and the number of splits are given as 10 and 2, respectively. Similarly, for the XGBoost model, the learning rate and the number of boosting stages are obtained as 0.1 and 100, respectively. Likewise, for the LGBM model, the learning rate and the depth of the tree are 0.2 and 15, respectively.

Moreover, the classification performance of the LGBM classifier with features from 5-s-duration-based LS signal frames has also been found. The accuracy of the LGBM is obtained as 68.33%, which is less than the accuracy value evaluated using the features of 4-s-duration LS signals. We have used mutual information (MI) [17] based feature selection or ranking approach for choosing 50 features out of 153

TABLE 2. Comparison of Accuracy of Proposed and Other Reported Methods

Feature extraction Method and Classifier	Ac_N(%)	Ac_P(%)	Ac_A(%)	OA(%)
MFCC features and KNN [10]	76.67	72.22	66.67	71.85
MFCC features and RF [10]	80.28	79.27	59.26	72.93
CNN with two convolution layers [10]	79.44	73.08	61.11	71.21
CNN with five convolution layers [10]	83.61	75.21	62.35	73.72
Proposed fixed boundary EWT domain selected features and LGBM	77.58	100	76.72	84.76

Ac_N, Ac_P, and Ac_A are accuracy values for normal, pneumonia, and asthma classes, respectively.

features of the LS signal. The accuracy values are reduced to 78.88%, 76.58%, 99.34%, and 74.15% for normal versus asthma, normal versus COPD, normal versus pneumonia, and four-class PD classification schemes using the LGBM classifier, respectively. The classification performance of the LGBM evaluated using all the 153 features and 50 selected features from LS signals for the normal versus pneumonia versus asthma classification scheme is 75.28 and 77.56%, respectively. Hence, the feature selection helped improve the classification accuracy of the LGBM classifier for the three-class classification scheme using LS signals.

In this letter, the time- and frequency-domain features are also evaluated using the DWT-based subband signals of the LS signal [18]. The number of decomposition levels for the DWT is considered as "9." The accuracy values of SVM, RF, XGBoost, and LGBM are obtained as 98.06, 99.63, 98.90, and 98.90%, respectively. The classification performance of classifiers is less using DWT-domain features than the EWT with the FBP-based features of LS signals. The proposed method is compared with the existing approaches for the normal versus pneumonia versus asthma classification strategy, and it is shown in Table 2. It is observed that the proposed approach provides the highest overall accuracy (OA) compared to MFCC-feature-based different classifiers and CNN models. The LGBM classifier coupled with FBP-based EWT domain features for pneumonia and asthma classes has obtained higher classification accuracy than that of the existing methods. The p-value less than 0.001 from the analysis of variance test [18] shows that the difference in the OA values of the proposed approach and the existing methods is statistically significant for detecting PDs. In CNN-based methods, rigorous training is needed to compute the data-driven features from LS signals to detect PDs [18]. The proposed method is simple and evaluates multiscale features from the LS signals to detect PDs using different classifiers. The computational complexity requirement of the FBP-based EWT is evaluated as $O[N\log(N)]$ [18], where N is the length of the LS signal. In the future, various optimization methods, such as genetic algorithm [19], improved particle swarm optimization [20], and artificial bee colony algorithm [21], can be used to select the relevant features of LS signals and parameters of classifiers to detect PDs.

V. CONCLUSION

An automated approach for the detection of PDs from LS signals was proposed in this letter. The EWT with the FBP was successfully employed to determine the modes of LS signals. The time- and frequency-domain features were evaluated from the modes of LS signals. These features were gainfully used for the automated detection of different PDs using machine learning models. The classification accuracy values of 80.35, 83.27, 99.34, and 77.13% were obtained for normal versus asthma, normal versus pneumonia, normal versus COPD, and classification of all the four classes, respectively. The proposed method can be tested using recorded LS signals in real time to detect PDs. In the future, the proposed feature-based classification models can be developed for the automated detection of other serious PDs using LS signals.

REFERENCES

[1] K. Nishio, T. Kaburagi, Y. Hamada, and Y. Kurihara, "Development of a bed-based unconstrained cardiac auscultation method," *IEEE Sens. Lett.*, vol. 5, no. 8, Aug. 2021, Art. no. 6001704.

[2] S. I. Khan and R. B. Pachori, "Automated classification of lung sound signals based on empirical mode decomposition," *Expert Syst. Appl.*, vol. 184, 2021, Art. no. 115456.

[3] A. Rao, E. Huynh, T. J. Royston, A. Kornblith, and S. Roy, "Acoustic methods for pulmonary diagnosis," *IEEE Rev. Biomed. Eng.*, vol. 12, pp. 221–239, 2018.

[4] R. Zulfiqar, F. Majeed, R. Irfan, H. T. Rauf, E. Benkhelifa, and A. N. Belkacem, "Abnormal respiratory sounds classification using deep CNN through artificial noise addition," *Front. Med.*, vol. 8, 2021, Art. no. 714811.

[5] R. Palaniappan, K. Sundaraj, and N. U. Ahamed, "Machine learning in lung sound analysis: A systematic review," *Biocybern. Biomed. Eng.*, vol. 33, no. 3, pp. 129–135, 2013.

[6] G. Serbes, S. Ulukaya, and Y. P. Kahya, "An automated lung sound preprocessing and classification system based onspectral analysis methods," in *Proc. Int. Conf. Biomed. Health Informat.*, 2017, pp. 45–49.

[7] N. Jakovljević and T. Lončar-Turukalo, "Hidden Markov model based respiratory sound classification," in *Proc. Int. Conf. Biomed. Health Informat.*, 2017, pp. 39–43.

[8] F. Demir, A. M. Ismael, and A. Sengur, "Classification of lung sounds with CNN model using parallel pooling structure," *IEEE Access*, vol. 8, pp. 105376–105383, 2020.

[9] D. Bardou, K. Zhang, and S. M. Ahmad, "Lung sounds classification using convolutional neural networks," *Artif. Intell. Med.*, vol. 88, pp. 58–69, 2018.

[10] L. Shi, K. Du, C. Zhang, H. Ma, and W. Yan, "Lung sound recognition algorithm based on VGGish-BIGRU," *IEEE Access*, vol. 7, pp. 139438–139449, 2019.

[11] R. Panda, S. Jain, R. Tripathy, and U. R. Acharya, "Detection of shockable ventricular cardiac arrhythmias from ECG signals using FFREWT filter-bank and deep convolutional neural network," *Comput. Biol. Med.*, vol. 124, 2020, Art. no. 103939.

[12] J. Gilles, "Empirical wavelet transform," *IEEE Trans. Signal Process.*, vol. 61, no. 16, pp. 3999–4010, Aug. 2013.

[13] B. Zhang, J. Ren, Y. Cheng, B. Wang, and Z. Wei, "Health data driven on continuous blood pressure prediction based on gradient boosting decision tree algorithm," *IEEE Access*, vol. 7, pp. 32423–32433, 2019.

[14] Z. Jiang *et al.*, "A light gradient boosting machine-enabled early prediction of cardiotoxicity for breast cancer patients," *Int. J. Radiat. Oncol., Biol., Phys.*, vol. 111, no. 3, 2021, Art. no. e223.

[15] M. Fraiwan, L. Fraiwan, B. Khassawneh, and A. Ibnian, "A dataset of lung sounds recorded from the chest wall using an electronic stethoscope," *Data Brief*, vol. 35, 2021, Art. no. 106913.

[16] G. Bonaccorso, *Machine Learning Algorithms*. Birmingham, U.K.: Packt, 2017.

[17] N. Hoque, D. K. Bhattacharyya, and J. K. Kalita, "MIFS-ND: A mutual information-based feature selection method," *Expert Syst. Appl.*, vol. 41, no. 14, pp. 6371–6385, 2014.

[18] P. Gajbhiye, N. Mingchinda, W. Chen, S. C. Mukhopadhyay, T. Wilaiprasitporn, and R. K. Tripathy, "Wavelet domain optimized Savitzky–Golay filter for the removal of motion artifacts from EEG recordings," *IEEE Trans. Instrum. Meas.*, vol. 70, 2020, Art. no. 4002111.

[19] W. Deng *et al.*, "An enhanced fast non-dominated solution sorting genetic algorithm for multi-objective problems," *Inf. Sci.*, vol. 585, pp. 441–453, 2022.

[20] G. Li, Y. Li, H. Chen, and W. Deng, "Fractional-order controller for course-keeping of underactuated surface vessels based on frequency domain specification and improved particle swarm optimization algorithm," *Appl. Sci.*, vol. 12, no. 6, 2022, Art. no. 3139.

[21] W. Deng, Z. Li, X. Li, H. Chen, and H. Zhao, "Compound fault diagnosis using optimized MCKD and sparse representation for rolling bearings," *IEEE Trans. Instrum. Meas.*, vol. 71, 2022, Art. no. 3508509.